Genetically Engineered DENV Produces Antigenically Distinct Mature Particles

Longping V. Tse[1,*], Rita M. Meganck[1], Stephanie Dong[1], Lily E. Adams [1,2], Laura J. White[2], Aravinda M. de Silva[2], Ralph S. Baric[1,2,*]

[1]Department of Epidemiology, [2]Department of Microbiology and Immunology,
The University of North Carolina at Chapel Hill, NC United States
* Co-corresponding authors: lvtse@med.unc.edu, rbaric@email.unc.edu

Abstract

Maturation of Dengue viruses (DENV) alters the structure, immunity and infectivity of the virion and highly mature particles represent the dominant form *in vivo*. The production of highly mature virions principally relies on the structure and function of the viral premature protein (prM) and its cleavage by the host protease furin. We developed a reliable clonal cell line which produces single-round mature DENVs without the need for DENV reverse genetics. More importantly, using protein engineering coupled with natural and directed evolution of the prM cleavage site, we engineered genetically stable mature DENVs without comprising viral yield and independent of cell, host, or passage. Using these complementary strategies to regulate maturation, we demonstrate that the resulting mature DENVs are antigenically distinct from their isogenic immature forms. Given the clinical importance of mature DENVs in immunity, our strategy provides a reliable strategy for the production of stable, high-titer mature candidate DENV live virus vaccines, genetically stabilized viruses for DENV maturation and immunity studies, and models for maturation-regulated experimental evolution in mammalian and invertebrate cells. Our data from directed-evolution across host species reveals distinct maturation-dependent selective pressures between mammalian and insect cells, which sheds light on the divergent evolutionary relationship of DENVs between its host and vector.

Introduction

Mosquito-borne Dengue virus (DENV) is a major global public health threat causing ~400 million new cases of dengue annually[1,2]. Although the majority of cases occur in tropical and subtropical areas where the mosquito vectors are most concentrated, global warming, travel, and globalization have contributed to the worldwide spread and intermixing of the four DENV serotypes[3]. Indeed, DENV infection has increased 30-fold between 1960 and 2010 with an upsurge of cases in the USA and Europe. A hallmark of DENV pathogenesis is the possibility for antibody dependent enhancement (ADE), which can progress to life threatening dengue hemorrhagic fever/dengue shock syndrome (DHF/DSS) upon secondary infection with a different serotype. So far, no antiviral treatments are available to treat DENV disease and the only approved vaccine, Dengvaxia, is not recommended for use in naïve populations[4,5].

Proteolytic cleavage of viral membrane fusion proteins is a common strategy for temporal or spatial control of virus infection, ultimately affecting tropism and transmission[6,7]. The DENV virion structural proteins consists of capsid, E (envelope), and prM glycoproteins which undergo major conformational changes via the process of maturation. The most common depiction of DENV particles features the mature form, which is composed of 90 Envelope (E) homodimers lying flat in a “herringbone” structure and organized into a 50 nm icosahedral (T=pseudo 3) symmetry resembling other non-enveloped virions[8]. However, the virion is assembled in the ER as a non-infectious[9], immature virion which adopts a completely distinct structure as a 60 nm “spikey” sphere with 60 three-fold spikes[10,11]. Each “spike” is composed of three E protein monomers elevated at a 27° upward angle with the fusion loop covered by prM proteins[11,12]. Maturation is a two-step process involving the proteolytic cleavage of prM by furin, a ubiquitously expressed serine protease with a preference for basic (positively charged) substrates, at the trans-Golgi network (TGN) followed by its release at neutral pH outside of the cell[11,13–15]. Cleavage of prM releases pr from the virion and triggers the E protein to rotate, ranging from ~137° to ~300°, to form the mature virion[10,16].

While the maturation status of common laboratory DENV strains varies, one study showed that clinical isolates are typically more mature, arguing the clinical importance of mature DENVs[17]. Because the E protein undergoes major conformational changes during processing, mature and immature virions are predicted to present dramatically different combinations of antigenic structures and epitopes[18,19]. Further complicating the process, the conformational change is reversible (“breathing”) and patchy, as a single particle can adopt both mature and immature forms in different regions and at different times[20]. The biological functions and characteristics of these heterogeneous maturation forms remain largely

unknown, but are thought to provide key evolutionary advantages in virus infection, immunity, and antigenic variation[21,22].

Previous studies have shown that fully mature DENV can be generated in Vero cells overexpressing furin[23]. However, due to the polyclonal nature of the cells, viral yield as well as maturity depends on the cell passage and culture conditions. Furthermore, maturation phenotypes quickly switch from mature back to immature after a single replication, which limits assay usage to those not requiring viral replication. Importantly, maturation status can vary significantly between serotypes and genotypes, suggesting the presence of other, less understood, regulatory determinants[24]. In this study, we develop two complementary strategies, ectopic expression of furin in culture and virus genetic engineering, to produce mature virions across the four DENV serotypes. Additionally, we provide insight into the role of variation in the prM furin cleavage site as the major molecular determinant governing DENV maturation in vertebrate and invertebrate cells. Using protein engineering and directed-evolution, we generated high yields of mature DENV1, 2 and 4 using unmodified Vero cells. The current study advances our understanding of the biological and genetic processes of DENV maturation, develops novel tools and recombinant viruses, and provides further insight and essential tools for future investigations.

Results

DENV Maturity is Serotype Dependent

DENV maturation regulates virion infectivity and antigenicity and directly impacts antibody neutralization and potential vaccine efficacy. Since furin cleavage of the prM protein initiates the DENV maturation process, we hypothesized that furin cleavage efficiency is directly proportional to DENV maturation. Consequently, we compared the DENV1-4 prM cleavage site with other mosquito-borne Flaviviruses, highly pathogenic avian influenza virus (HPAI) and SARS-CoV-2. Sequence analyses suggested that all the DENV serotypes encoded a sub-optimal furin cleavage site (P4) R-X-K/R-R (P1) with negative modulators as indicated by an acidic residue at the P3 position (Fig. 1a). To analyze the functionality of the prM furin cleavage site in a more quantitative manner, we used the computational program PiTou, which combines machine learning and cumulative probability score function of known furin cleavages to calculate the logarithmic-odd probabilities of all the different viral furin cleavage sites[25]. These analyses provided strong predictive data that the DENV serotypes encode suboptimal furin sites (scores from 6.90 – 13.26) compared with other Flaviviruses (scores from 13.30 – 15.40) (Fig. 1a). We focused our studies on four prototypical wildtype (WT) DENV viruses including WestPac (DV1-WT), S16803 (DV2-WT), 3001 (DV3-WT) and Sri Lanka 92 (DV4-WT) isolates (Table 1). Using western blotting as a readout, we

89 determined the relative maturity of each serotype by calculating the ratio of prM to E. Consistent with
90 the hypothesis that prM cleavage is dependent on both local primary sequence and other distal and
91 structural functions, PiTou predictions do not translate completely to the empirical maturation status of
92 DENV. Relative maturity was clearly different between serotypes. In particular, serotypes encoding an
93 Glutamic acid (E), but not Aspartic acid (D) at the P3 position (prM residue 89) are associated with more
94 immature virion production in Vero cells, with DV2-WT virions containing the highest level of uncleaved
95 prM, followed by DV4-WT, DV3-WT, and DV1-WT which has nearly undetectable levels of prM, and hence
96 is more mature (Fig. 1b).

Serotype	Strain	Genotype
DV1	WestPac 74 (WHO)	IV
DV2	S16803 (WHO)	Asian I
DV3	3001	III
DV4	Sri Lanka 92	IIb

Table 1: Prototypic WT DENV strains used in this study.

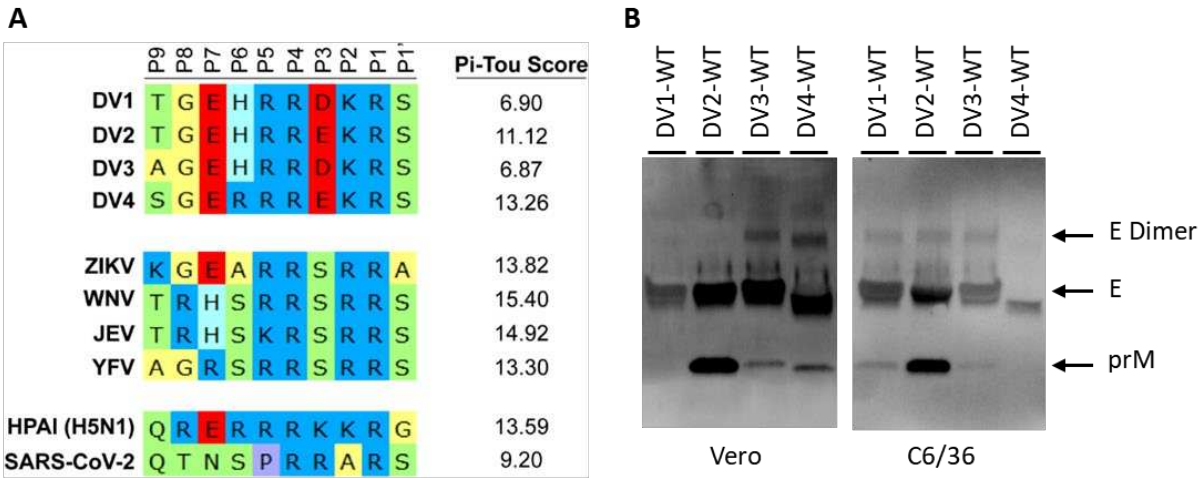

97

98 **Figure 1**: Furin cleavage site alignment and DENV maturation. (A) Amino acid sequence alignment of viral
99 furin cleavage sites from position 9 (P9) to position 1 prime (P1'). Pi-Tou scores are the prediction of
100 logarithmic-odd probabilities of all the different viral furin cleavage sites (higher value = better substrate
101 for furin). DENV1, 2, 3 4, Zika virus (ZIKV), West Nile virus (WNV), Japanese encephalitis virus (JEV), yellow
102 fever virus (YFV), highly pathogenic avian influenza virus (HPAI) and SARS-Coronavirus-2. (B)
103 Representative western blot images of DENV 1-4 viral supernatants from Vero and C6/36 cells blotted
104 with anti-Env and anti-prM antibodies.

105

Optimized Clonal Vero-furin Cells Generate High Yield, Mature DENV

DENV maturation also depends on the producer cells; for instance, C6/36 grown DENVs show a different maturation profile, from DV2-WT (most immature) < DV1-WT = DV3-WT < DENV4 (most mature) (Fig. 1b). As reported previously[23], fully mature DENV strains can be generated in Vero cells that overexpress furin. However, high level furin expression may negatively impact DENV virus production. Using the sleeping beauty transposon system[26], we isolated two clonal lines with high (VF-Hi) or low (VF-Lo) levels of furin expression (Fig. 2a). Immunofluorescent staining and western blot analysis revealed different levels of furin expression in the trans-Golgi network (Fig. 2b and 2c). The growth kinetics of all four DENV serotypes were tested on both Vero-furin lines and compared to unmodified Vero cells (Fig. 2d – g). DV1-WT, DV2-WT and DV4-WT showed similar growth kinetics in all cell lines tested, while VF-Hi supported better DV3-WT growth (Fig. 2d – g). VF-Hi supports the production of fully mature DENV virions across all four serotypes (Fig. 2d – g). In agreement with the low furin expression level, VF-Lo phenocopied the DENV maturation status of unmodified Vero cells (Fig. 2d – g). Therefore, VF-Hi cells allow for high DENV yield in all serotypes, suggesting the furin expression level in VF-Hi is optimal for production of fully mature DENVs.

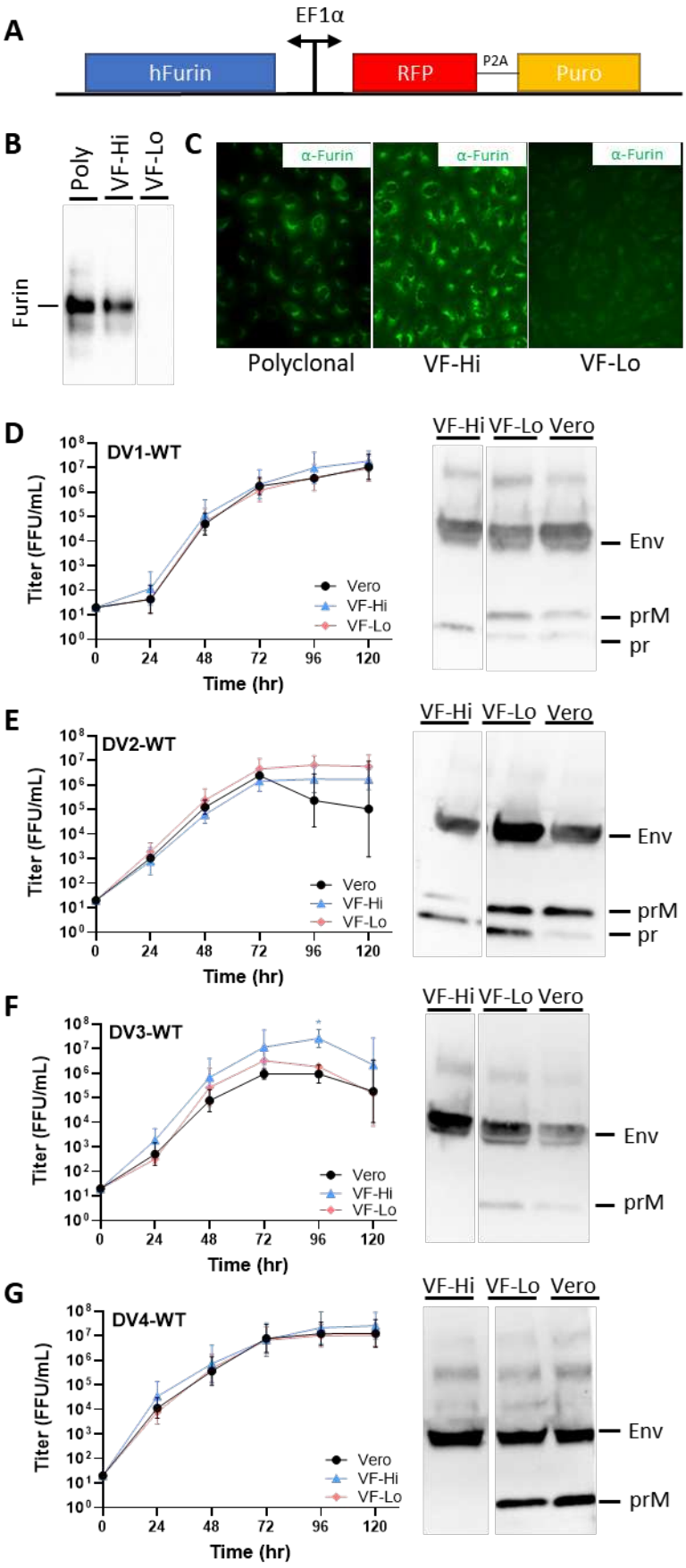

Figure 2: Growth kinetics and maturation status of Vero-furin grown DENVs. (A) Schematic of the Sleeping Beauty-based transposon cassette for ectopic expression of human furin (hFurin). A bi-directional EF1a promoter was used to drive the expression of hFurin and red-fluorescent protein (RFP) with a puromycin resistance gene (Puro) linked by a 2A self-cleaving peptide (P2A). (B) Western blot and (C) immunofluorescence images of polyclonal and clonal selected high (VF-Hi) and low (VF-Lo) expression hFurin Vero cells using anti-furin antibodies. Growth kinetics and degree of maturation of (D) DENV1-WT, (E) DENV2-WT, (F) DENV3-WT and (G) DENV4-WT in unmodified Vero cells (Black-Circle), VF-Hi cells (Blue-Triangle) and VF-Lo cells (Pink-Diamond). Cells were infected with DENV at MOI 0.01 – 0.05 for 120 hours. Supernatants were harvested at 120hpi and analyzed by western blot for DENV maturation using anti-Env and anti-prM antibodies. All assays were performed with at least two biological repeats with two technical replicates. Growth kinetics of DENV variants were compared to their corresponding wildtype using 2-way ANOVA multiple comparisons.

Genetic Regulation of DENV1 and DENV4 Maturation Status

As an alternative to ectopic overexpression of furin which only generates mature virion for a single round of infection, we hypothesized that genetic modification of the prM furin cleavage site could also be used to optimize DENV maturation independence of cells or hosts. Using DV1-WT as a model, we introduced a mutation at the P3 position of the furin cleavage site and generated an isogenic strain, DV1-prM-D89K. The mutated cleavage site (HRRKKR|S) has a Pi-Tou score of 14.68 compared to the DV1-WT cleavage site (HRRDKR|S) with a Pi-Tou score of 6.90, predicting more optimal cleavage (Fig. 3a). DV1-WT and DV1-prM-D89K displayed no difference in virus growth kinetics in Vero (mammalian) and C6/36 (insect) cells (Fig. 3b). In both Vero and C6/36 cultures, DV1prM-D89K was more mature than DV1-WT, phenocopying the Vero-furin grown DV1-WT (Fig. 3c).

To understand if the furin cleavage site mutation is portable across serotypes, we introduced a similar mutation on the DV4-WT backbone, generating the isogenic strain DV4-prM-E89K (Fig. 3d). While we successfully generated a pure population of DV4-prM-E89K in C6/36 cells, a spontaneous mutation, K89N, rapidly emerged and gave rise to a new evolved DV4-prM-E89N variant in Vero cells by passage 2 (Fig. S1a). By the 5th passage, the DV4-prM-E89N variant represented 100% of the viral population (Fig. S1a), supporting the notion that viruses encoding the E89K mutation were less fit than those encoding the E89K mutation in Vero cells. Growth kinetics of DV4-prM-E89K and DV4-prM-E89N on C6/36 cells are comparable to DV4-WT (Fig. 3e). However, the DV4-prM-E89K variant displayed a robust 2-log growth defect compared to DV4-prM-E89N and DV4-WT on Vero cells (Fig. 3f). When grown at 32°C, the growth

154 defect of DV4-prM-E89K was alleviated (Fig. S1c). The maturation status of the two variants were tested
155 and compared to DV4-WT. DV4-prM-E89N is more mature than DV4-WT in both Vero and C6/36 cells (Fig.
156 3g). No prM can be detected in DV4-prM-E89K; due to the low virus yield in Vero cells, the data suggest
157 that either DV4-prM-E89K is fully mature or the protein input is below detection limit (Fig. S1b). As
158 calculated by Pi-Tou, DV4 has the highest furin cleavage score among the DENV serotypes at 13.26. The
159 point mutation prM-E89K increases the score to 16.65 (the highest score observed), while DV4-prM-E89N
160 has a Pi-Tou score of 13.82 (Fig. 3d). In DENV4, it seems that a ”super-optimal” furin cleavage site may
161 negatively impact DENV growth in Vero cells. The data suggest a delicate balance likely exists between
162 virion maturation, furin cleavage site efficiency, and viral fitness in different serotypes.

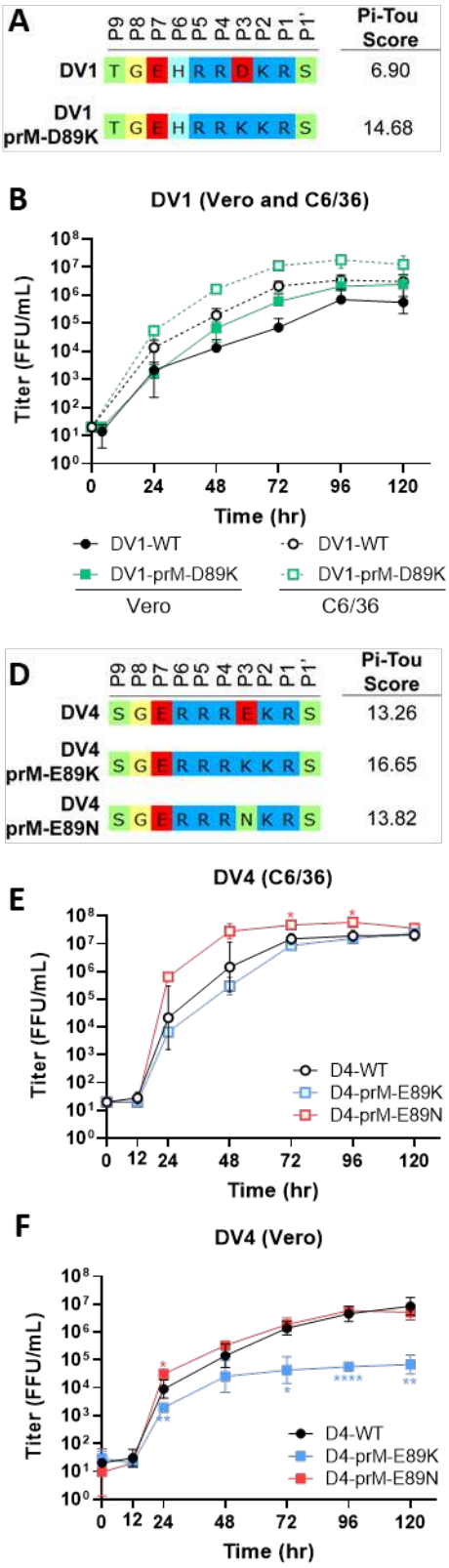

Figure 3: Generation of mature DENV1 and DENV4 via genetic modification. (A) Sequence alignment and Pi-Tou scores of DV1-WT and DV1-prM-D89K. (B) Growth kinetics of DV1-WT and DV1-prM-D89K in Vero and C6/36 cells. (C) Representative western blot image (bottom) of DV1-WT and DV1-prM-D89K viral supernatants blotted with anti-Env and anti-prM antibodies, and quantification (top) of viral maturation (prM/Env) normalized to DV1-WT (lower value = more mature). (D) Sequence alignment and Pi-Tou scores of DV4-WT, DV4-prM-E89K and DV4-prM-E89N. Growth kinetics of DV4-WT, DV4-prM-E89K and DV4-prM-E89N in (E) C6/36 and (F) Vero cells. (G) Representative western blot image (bottom) of DV4-WT, DV4-prM-E89K and DV4-prM-E89N viral supernatants blotted with anti-Env and anti-prM antibodies and quantification (top) of viral maturation (prM/Env) normalized to DV4-WT (lower value = more mature). Growth kinetics and maturation of DENV variants were compared to their corresponding wildtype using 2-way ANOVA multiple comparisons.

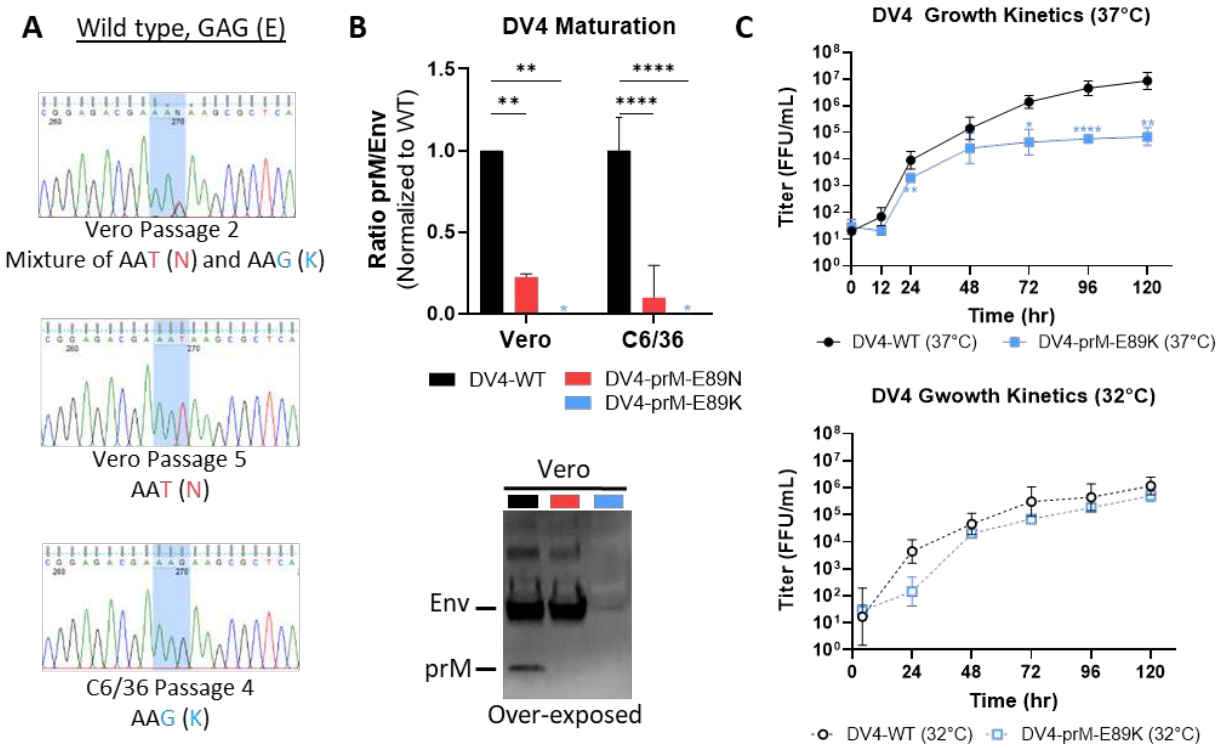

Supplementary Figure 1: (A) DNA Chromatograms of DV4-E89K in C6/36 cells (bottom) as well as Vero cells from early (P2, top) and late (P5, middle) passage. (B) Representative western blot image (bottom) of DV4-WT, DV4-prM-E89K and DV4-prM-E89N viral supernatant blotted with anti-Env and anti-prM antibodies, and quantification of viral maturation (prM/Env) normalized to DV4-WT. (C) Growth kinetics of DV4-WT and DV4-prM-E89K in Vero and C6/36 cells at 32ºC (bottom) and 37ºC (top).

Directed Evolution Reveals High Levels of Plasticity in DENV2 prM Cleavage Site

Based on the spontaneous K89N mutation in DV4, we hypothesized the prM cleavage site has high plasticity, suggesting the existence of a "Goldilocks Zone" for efficient *in vitro* growth. We utilized saturation mutagenesis and directed-evolution to simultaneously screen thousands of DENV2 prM cleavage site variants for efficient growth in tissue culture. We generated a DENV2 viral library in which four positions, P3, P5, P6, and P7, of the prM cleavage site were randomly mutated, preserving the core furin cleavage site (Fig. 4a). The library was propagated three times in either Vero or C6/36 cells, and each passage of the virus were deep sequenced along with the plasmid library (Fig. 4a). The theoretical amino acid diversity of the library is 160,000 variants (ignoring stop codons), which was represented in the plasmid library (Table 2). As expected, viral diversity rapidly drops after one passage, to 0.7% (1148 unique variants) and 16.2% (25942 unique variants) of the theoretical maximum in Vero and C6/C6 respectively, further diminished after each passage (Table 2). The large number of viable DENV2 variants in both cells indicates a high degree of plasticity within the prM cleavage site in culture (Table 2). Importantly, C6/36 cells were more tolerant to prM cleavage site variations than Vero, suggesting a higher selective pressure exerted by mammalian cells. After three rounds of selection in C6/36 and Vero cells, two different dominant variants, TGRAQRYKR|S (DV2-C1) and TGAGRRSKR|S (DV2-V1), emerged, representing almost 50% of their respective viral populations (Fig 4b and 4c). While the DV2-WT cleavage site has a Pi-Tou score of 11.12, the Vero-selected cleavage site score increased to 14.39. Surprisingly, the DV2-C1 cleavage site scored at 7.76, a much lower score than DV2-WT (Fig. 4d). We plotted the PiTou score distribution of the top 50 ranked variants in C6/36 and Vero cells, with peaks at 7.7 and 14.9, respectively (Fig. 4e). We also plotted the Pi-Tou scores of the top 50 sequences from passage 1 that were extinct by passage 3. Although there was no distinct peak of deselection in C6/36 cells, a distinct peak of Pi-Tou scores at 13.9 were observed in the Vero-selected extinct population (Fig. 4e). The sequences, counts, and Pi-Tou scores of the top 50 enriched and deselected cleavage sites are summarized in Table S1 and S2. Due to founder effects in directed-evolution experiments, there is only one sequence shared between the top 50 variants evolved from Vero and C6/36 cells after three passages. Additionally, some variants with high Pi-Tou scores are rapidly deselected in both Vero and C6/36 cells, suggesting that the furin cleavage site sequence plays multiple roles in viral fitness (Table S2). The difference in scores between the two cell lines and the leveling effect of the lower ranked variants highlighted the differential fitness requirements of DENV2 between insect and mammalian cells.

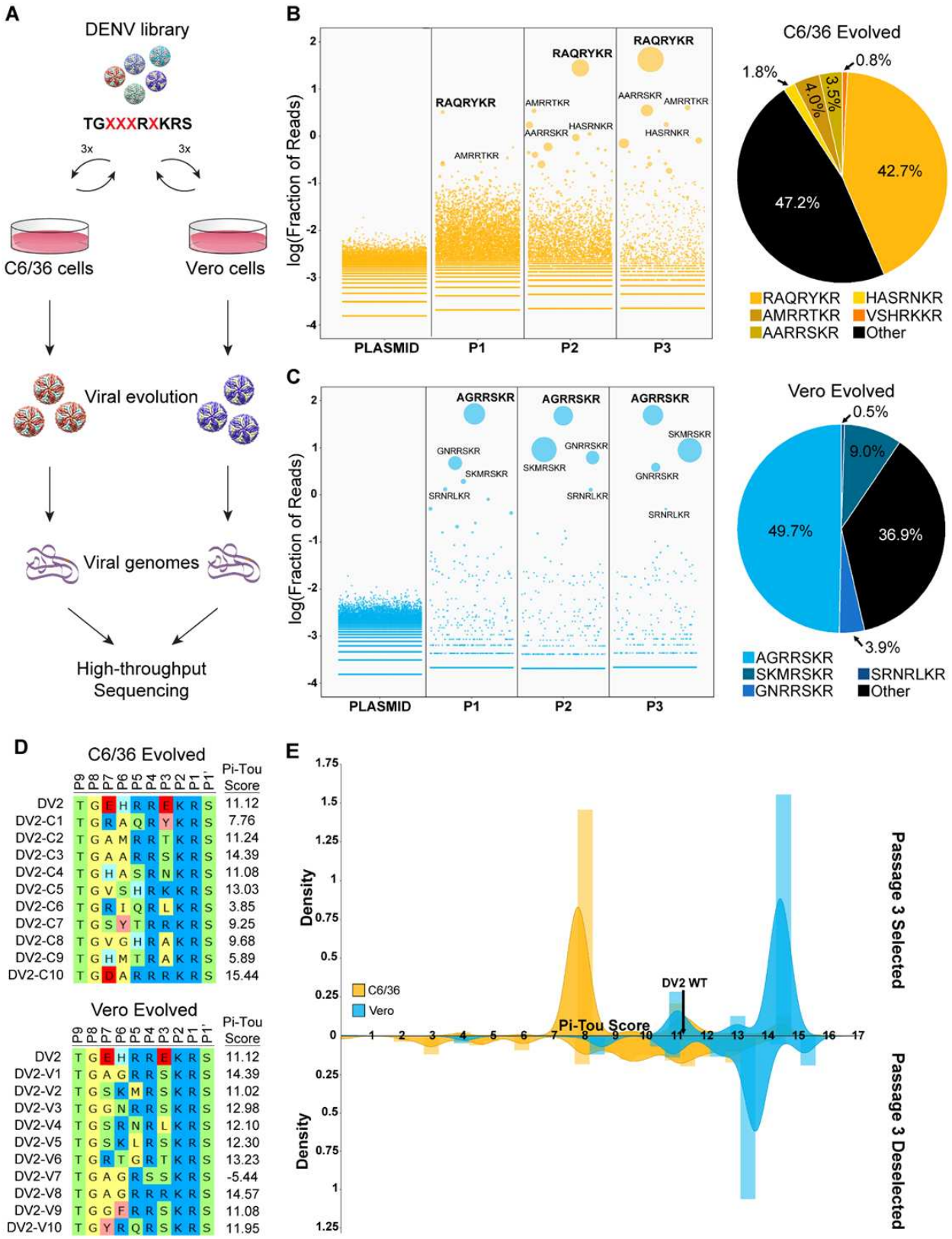

Figure 4: Directed-evolution of DENV2 prM cleavage site in Vero and C6/36 cells. (A) Schematic of directed-evolution from library generation to high-throughput sequencing. Enrichment plot of prM

cleavage site sequences from plasmid library to viral population at the 3rd passage (P3) and the proportion as well as sequence of the Top 5 enriched sequences in (B) C6/36 (yellow) and (C) Vero cells (Cyan). (D) Sequences and Pi-Tou scores of the Top 10 enriched prM cleavage sites from C6/36 and Vero cells. (E) Top: Distribution plot of Pi-Tou scores from the top 50 enriched prM cleavage sites in the 3rd passage of C6/36 (yellow) and Vero cells (Cyan). PiTou score of DV2-WT is marked at 11.12 with a dark line. Bottom: Distribution plot of Pi-Tou scores of the top 50 variants present at the 1st passage but lost in the 3rd passage of C6/36 (yellow) and Vero cells (Cyan).

Name	Sequence	Pi-Tou Score			Name	Sequence	Pi-Tou Score
DENV2-C1	TGRAQRYKRS	7.33832			DENV2-V1	TGAGRRSKRS	14.843
DENV2-C2	TGAARRSKRS	14.843			DENV2-V2	TGGNRRSKRS	13.4061
DENV2-C3	TGAAVRSKRS	12.3488			DENV2-V3	TGSKMRSKRS	11.3468
DENV2-C4	TGAMRRTKRS	11.6874			DENV2-V4	TGSRNRLKRS	12.4246
DENV2-C5	TGRIQRLKRS	3.4267			DENV2-V5	TGMAKRSKRS	13.7489
DENV2-C6	TGNSGRHKRS	11.4735			DENV2-V6	TGTAKRSKRS	13.7489
DENV2-C7	TGFSTRNKRS	10.0498			DENV2-V7	TGYRQRSKRS	12.3466
DENV2-C8	TGAANRVKRS	11.1661			DENV2-V8	TGLSRRSKRS	15.3795
DENV2-C9	TGSVQRIKRS	8.36797			DENV2-V9	TGGFRRSKRS	11.508
DENV2-C10	TGVSRRSKRS	15.3795			DENV2-V10	TGRQARSKRS	11.0661
DENV2-C11	TGSTRRDKRS	7.72902			DENV2-V11	TGKMRREKRS	8.66191
DENV2-C12	TGTKGRVKRS	12.3958			DENV2-V12	TGSNKRHKRS	10.7461
DENV2-C13	TGTTHRHKRS	11.0362			DENV2-V13	TGRTGRTKRS	12.8044
DENV2-C14	TGLPVRSKRS	12.6207			DENV2-V14	TGERARVKRS	12.8337
DENV2-C15	TGSRTRSKRS	13.0648			DENV2-V15	TGRYKRDKRS	4.10841
DENV2-C16	TGSTRRHKRS	13.4014			DENV2-V16	TGAGRSSKRS	-4.9918
DENV2-C17	TGHVSRSKRS	12.2249			DENV2-V17	TGAWRRSKRS	-5.18386
DENV2-C18	TGTRNRKKRS	13.8726			DENV2-V18	TGAGRRRKRS	15.0224
DENV2-C19	TGFTNRVKRS	11.247			DENV2-V19	TGGKSRVKRS	13.5558
DENV2-C20	TGSNSRSKRS	12.156			DENV2-V20	TGRPVRSKRS	12.6207
DENV2-C21	TGASSRHKRS	12.598			DENV2-V21	TGHSRREKRS	12.5334
DENV2-C22	TGQVHRSKRS	11.0663			DENV2-V22	TGWGKRSKRS	13.7489
DENV2-C23	TGTAKRSKRS	13.7489			DENV2-V23	TGTGRRMKRS	12.5588
DENV2-C24	TGNLRRTKRS	14.5679			DENV2-V24	TGAGRRIKRS	13.5353
DENV2-C25	TGFSSRSKRS	14.164			DENV2-V25	TGRSKRSKRS	14.2854
DENV2-C26	TGGKVRNKRS	10.82			DENV2-V26	TGSVRRVKRS	12.5076
DENV2-C27	TGGHVRHKRS	10.4826			DENV2-V27	TGASHRSKRS	13.016
DENV2-C28	TGSAQRSKRS	11.1173			DENV2-V28	TGMSKRTKRS	14.4649
DENV2-C29	TGEKKRAKRS	11.8098			DENV2-V29	TGAGRRNKRS	12.5588
DENV2-C30	TGITTRSKRS	11.6576			DENV2-V30	TGPGRRSKRS	14.843
DENV2-C31	TGAHKREKRS	10.4483			DENV2-V31	TGFKHRVKRS	12.2057
DENV2-C32	TGGARRQKRS	14.399			DENV2-V32	TGGRHRNKRS	11.2579
DENV2-C33	TGLTRRSKRS	14.9674			DENV2-V33	TGAGSRSKRS	13.6629
DENV2-C34	TGASRRAKRS	13.0953			DENV2-V34	TGAGLRSKRS	11.8703
DENV2-C35	TGHMTRAKRS	6.18586			DENV2-V35	TGAARRSKRS	14.843
DENV2-C36	TGLKVRHKRS	11.5383			DENV2-V36	TGAGRRTKRS	15.0224
DENV2-C37	TGGAKRGKRS	10.9028			DENV2-V37	TGAERRSKRS	11.508
DENV2-C38	TGHASRNKRS	11.3823			DENV2-V38	TGSKLRSKRS	12.6269
DENV2-C39	TGGDARRKRS	9.84567			DENV2-V39	TGAVRRSKRS	13.4061
DENV2-C40	TGVASRTKRS	13.846			DENV2-V40	TGTGRRSKRS	14.843
DENV2-C41	TGNYPRNKRS	7.18517			DENV2-V41	TGARRRSKRS	15.626
DENV2-C42	TGERTRSKRS	13.0648			DENV2-V42	TGATKRSKRS	13.8734
DENV2-C43	TGRRMRSKRS	11.7847			DENV2-V43	TGDGRRSKRS	14.843
DENV2-C44	TGERKRAKRS	12.2477			DENV2-V44	TGSKIRTKRS	13.2837
DENV2-C45	TGMNKRSKRS	12.312			DENV2-V45	TGAGCRSKRS	-5.14866
DENV2-C46	TGHPSRGKRS	11.0941			DENV2-V46	TGSGRRSKRS	14.843
DENV2-C47	TGVRARTKRS	13.9117			DENV2-V47	TGGTRRSKRS	14.9674
DENV2-C48	TGRSLRSKRS	12.3732			DENV2-V48	TGVGRRSKRS	14.843
DENV2-C49	TGMPRRSKRS	15.082			DENV2-V49	TGISKRGKRS	11.1775
DENV2-C50	TGRAVRHKRS	10.7828			DENV2-V50	TGSRNRFKRS	11.0389

Supplemental Table 1: Top 50 enriched sequences and PiTou scores of DV2 directed-evolution.

Name	Sequence	Pi-Tou Score			Name	Sequence	Pi-Tou Score
DENV-DC1	TGQNSRLKRS	11.2574			DENV-DV1	TGMAKRSKRS	13.7489
DENV-DC2	TGQMSRNKRS	8.01577			DENV-DV2	TGTAKRSKRS	13.7489
DENV-DC3	TGSNYRSKRS	4.65351			DENV-DV3	TGLSRRSKRS	15.3795
DENV-DC4	TGLFTRNKRS	6.15277			DENV-DV4	TGRQARSKRS	11.0661
DENV-DC5	TGRLRRAKRS	12.1042			DENV-DV5	TGKMRREKRS	8.66191
DENV-DC6	TGTPKRLKRS	13.0894			DENV-DV6	TGSNKRHKRS	10.7461
DENV-DC7	TGKINRAKRS	2.98847			DENV-DV7	TGERARVKRS	12.8337
DENV-DC8	TGSFTRSKRS	8.43697			DENV-DV8	TGRYKRDKRS	4.10841
DENV-DC9	TGGSPRAKRS	10.126			DENV-DV9	TGGKSRVKRS	13.5558
DENV-DC10	TGSKLRIKRS	11.3193			DENV-DV10	TGRPVRSKRS	12.6207
DENV-DC11	TGTGTRLKRS	10.9346			DENV-DV11	TGHSRREKRS	12.5334
DENV-DC12	TGHMNRLKRS	7.79803			DENV-DV12	TGWGKRSKRS	13.7489
DENV-DC13	TGFSTRQKRS	11.8901			DENV-DV13	TGTGRRMKRS	12.5588
DENV-DC14	TGGTTRAKRS	9.63526			DENV-DV14	TGRSKRSKRS	14.2854
DENV-DC15	TGESMRSKRS	11.0639			DENV-DV15	TGSVRRVKRS	12.5076
DENV-DC16	TGYRSRPKRS	13.0114			DENV-DV16	TGASHRSKRS	13.016
DENV-DC17	TGSNSRAKRS	9.87178			DENV-DV17	TGMSKRTKRS	14.4649
DENV-DC18	TGRSIRSKRS	12.8553			DENV-DV18	TGFKHRVKRS	12.2057
DENV-DC19	TGHDSRHKRS	9.20017			DENV-DV19	TGGRHRNKRS	11.2579
DENV-DC20	TGFVGRHKRS	9.53267			DENV-DV20	TGATKRSKRS	13.8734
DENV-DC21	TGGAHRLKRS	11.6078			DENV-DV21	TGISKRGKRS	11.1775
DENV-DC22	TGSNPRMKRS	8.12156			DENV-DV22	TGNHRRNKRS	12.1042
DENV-DC23	TGSNTRIKRS	9.01827			DENV-DV23	TGSLRRIKRS	13.0807
DENV-DC24	TGVTARTKRS	12.808			DENV-DV24	TGQYKRSKRS	11.3468
DENV-DC25	TGTRVRSKRS	13.5421			DENV-DV25	TGRPRRDKRS	7.84358
DENV-DC26	TGHVGRDKRS	3.86024			DENV-DV26	TGYSKRPKRS	12.4046
DENV-DC27	TGSIMRHKRS	2.208			DENV-DV27	TGMAQRSKRS	11.1173
DENV-DC28	TGPKSRLKRS	13.5558			DENV-DV28	TGTSRRNKRS	13.0953
DENV-DC29	TGNVRRYKRS	9.62714			DENV-DV29	TGQKARSKRS	13.2943
DENV-DC30	TGYSRRDKRS	8.14108			DENV-DV30	TGIAKRSKRS	13.4871
DENV-DC31	TGYGHRYKRS	8.72497			DENV-DV31	TGGRTRQKRS	12.6208
DENV-DC32	TGAANRLKRS	11.1661			DENV-DV32	TGRKVRSKRS	13.1042
DENV-DC33	TGVHNRNKRS	9.49747			DENV-DV33	TGSMKRSKRS	10.4139
DENV-DC34	TGVTARLKRS	11.73			DENV-DV34	TGTAQRSKRS	11.1173
DENV-DC35	TGHNTRDKRS	3.08753			DENV-DV35	TGNTHRTKRS	12.7816
DENV-DC36	TGASHRPKRS	11.1351			DENV-DV36	TGGFRRYKRS	7.72902
DENV-DC37	TGGTRRVKRS	14.0689			DENV-DV37	TGNKSRNKRS	12.1701
DENV-DC38	TGVPMRQKRS	10.3953			DENV-DV38	TGKTRRDKRS	7.72902
DENV-DC39	TGSGNRAKRS	9.77666			DENV-DV39	TGMTRRGKRS	12.1213
DENV-DC40	TGKIGREKRS	2.90178			DENV-DV40	TGRHRRDKRS	7.15001
DENV-DC41	TGHHNRTKRS	11.9611			DENV-DV41	TGTSRRHKRS	13.8135
DENV-DC42	TGWTARSKRS	12.6286			DENV-DV42	TGQNRRDKRS	6.16771
DENV-DC43	TGSKIRDKRS	5.86584			DENV-DV43	TGMAKRTKRS	13.9284
DENV-DC44	TGLHGRPKRS	10.3586			DENV-DV44	TGTAKRLKRS	12.8504
DENV-DC45	TGTAGRNKRS	10.2558			DENV-DV45	TGSLSRHKRS	11.6436
DENV-DC46	TGDQRRLKRS	12.5076			DENV-DV46	TGLSKRSKRS	14.2854
DENV-DC47	TGRTHRFKRS	10.318			DENV-DV47	TGASRRDKRS	8.14108
DENV-DC48	TGGFGRSKRS	9.14369			DENV-DV48	TGSKNRAKRS	10.601
DENV-DC49	TGHSYRPKRS	4.78077			DENV-DV49	TGSRVRDKRS	6.30372
DENV-DC50	TGERWRHKRS	-5.40603			DENV-DV50	TGDTRRSKRS	14.9674

Supplemental Table 2: Top 50 deselected sequences and PiTou scores of DV2 directed-evolution

The top ranked evolved variants, DV2-V1 and DV2-C1, were re-derived via reverse genetics for further characterization. We also included a DV2-prM-E89K variant similar to the original DV1 mutation as comparison (Fig. 5c). While the DV2-prM-E89K variant has slightly reduced growth in Vero cells compared to DV2-WT, both DV2-V1 and DV2-C1 grow better than DV2-WT in Vero, with a drop in titer in C6/36 cells at 96 to 120 hpi (Fig. 5a and 5b). In Vero cells, DV2-prM-E89K and DV2-V1 are almost fully mature while DV2-C1 is only 30% more mature than DV2 WT (Fig. 5d). When the viruses are grown in C6/36, all the variants are 60 – 70% more mature than DV2 WT (Fig. 5d).

	C6/36 Evolved		Vero Evolved	
	Unique Sequences	% Maximum	Unique Sequences	% Maximum
Plasmid	164569	102.86*	164569	102.86*
P1	25942	16.21	1148	0.72
P2	14119	8.82	719	0.45
P3	6026	3.77	683	0.43

* Plasmid library contains some sequences with stop codons.

Table 2: Summary of plasmid and viral passages diversities of DV2 directed-evolution.

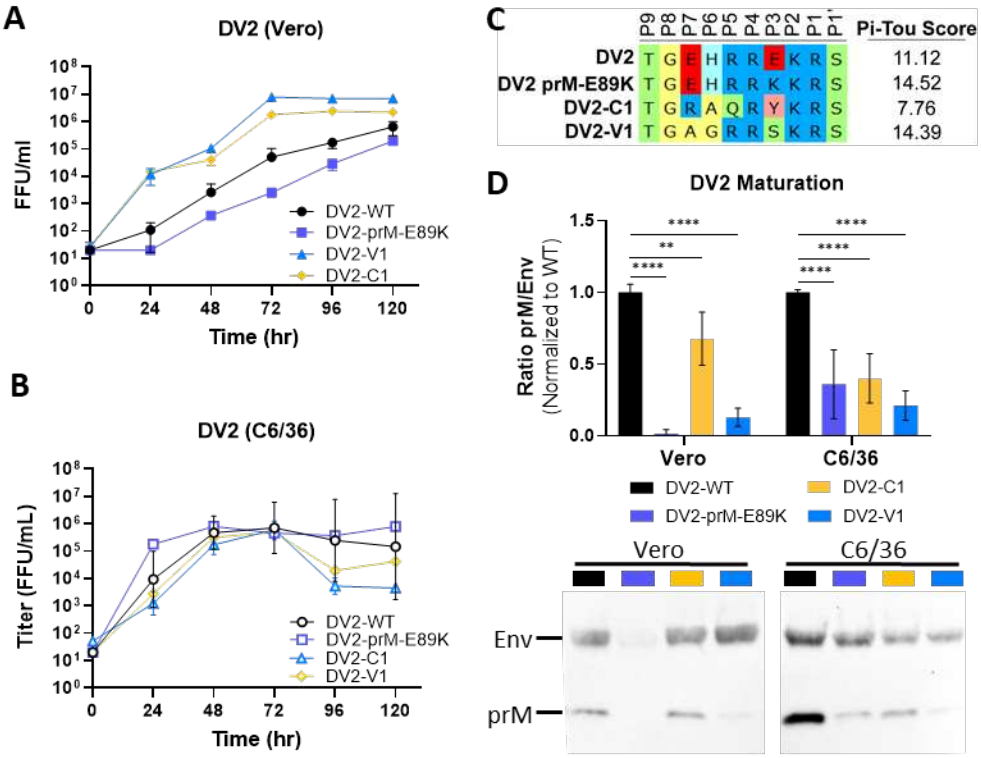

Figure 5: Generation of mature DENV2 via directed-evolution. Growth kinetics of DV2-WT, DV2-prM-E89K, DV2-C1 and DV2-V1 in (A) Vero and (B) C6/36 cells. (C) Sequence alignment and PiTou scores of DV2-WT, DV2-prM-E89K, DV2-C1 and DV2-V1 (D) Representative western blot image (bottom) of DV2-WT, DV2-

prM-E89K, DV2-C1, and DV2-V1 viral supernatants blotted with anti-Env and anti-prM antibodies, and quantification (top) of viral maturation (prM/Env) normalized to DV2-WT (lower value = more mature). Growth kinetics and maturation of DV2 variants were compared to DV2-WT using 2-way ANOVA multiple comparisons.

Impact of Maturation Status on DENV Epitope Presentation and Antigenicity

Given the ability to generate fully mature DENVs, we next evaluated the impact of maturation status on antigenicity. We selected several monoclonal antibodies targeting different regions of the DENV E glycoprotein, including C10 (Envelope-Dimer-Epitope 1)[27], B7 (Envelope-Dimer-Epitope 2)[27], 1C19 (BC loop)[28] and 1M7 (fusion loop)[28]. As expected, Ab epitopes that are not maturation dependent are preserved, as evidenced by antibodies such as C10, B7, and 1C19 which showed no difference in Foci Reduction Neutralization Titer 50 values (FRNT50) (Fig. 6a – c). However, the fusion loop targeting antibody 1M7 showed significantly different FRNT50 values between fully mature and less mature DENVs in DENV1 and 4, but not in DENV2 (Fig. 6a – c). For DENV4, we also tested polyclonal sera from patients 180 days post DENV4 vaccination or naturally infected patients from a traveler cohort. Polyclonal serum contains a mixture of antibodies which may or may not be affected by virion maturation status. Unsurprisingly, $FRNT_{50}$ of polyclonal serum was equivalent for fully mature and partially mature DENV4 (Fig. 6d).

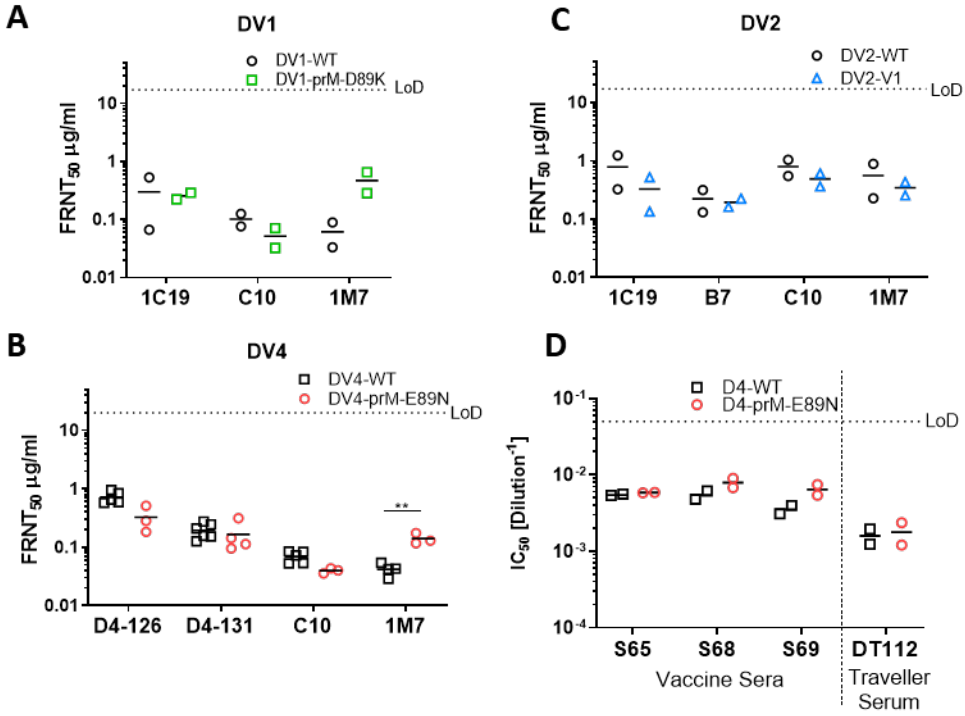

Figure 6: Antigenic profile of mature DENV. (A) $FRNT_{50}$ of DV1-WT and DV1-prM-D89K against 1C19, EDE1-C10 (C10) and 1M7. (B) $FRNT_{50}$ of DV4-WT and DV4-prM-E89N against D4-126, D4-131, C10 and 1M7. (C) $FRNT_{50}$ of DV2-WT and DV2-V1 against 1C19, EDE2-B7 (B7), C10 and 1M7. (D) $FRNT_{50}$ of vaccine sera and traveler serum against DV4 and DV4-prM-E89N.

Discussion

In this report, we provided two methods to produce fully mature DENVs, and demonstrated that the prM furin cleavage site is the main determinant of maturation. The minimal furin cleavage site only requires (P4) R-X-K/R-R (P1), but cleavage efficiency greatly depends on positions P7, P6, P5, P3 and P1' – P4'[29–31]. Algorithms such as Pi-Tou (used here) and ProP utilize machine learning to predict furin cleavage site efficiency while Pi-Tou also account for cumulative probability score function of known furin cleavage[25,32]. It must be noted that both programs focus on mammalian furin rather than invertebrate furin proteases; human furin and *Aedes aegypti* furin-like-proteases only share ~40% sequence identity (Fig. S2) and Drosophila furin has been shown to have different substrate preferences[33]. Perhaps unsurprisingly, Pi-Tou predictions do not correlate fully with DENV maturation, as other determinants such as cleavage site accessibility, protein structure, stability, and the stem region of prM can also affect maturation in DENV and other viruses[34–36]. In DENV4, the degree of maturation differs among genotypes with identical prM proteins, suggesting contributions by an envelope-dependent maturation determinant as well[24]. A previous study generated mature dengue virus-like-particles (VLPs) by modifying the prM cleavage site for optimal cleavage[37]. In the current work, modification of the furin cleavage site and removal of the acidic P3 residues generated fully mature live DENV1, 2, and 4. However, unlike with Dengue-VLPs, experiments with authentic virus exposed the fitness cost of these mutations. The large growth defect of the DV4-prM-E89K variant was alleviated by reducing the temperature from 37°C to 32°C during virus production, indicating that the mutation impacts stability[18], while the spontaneous mutation K89N restored viral fitness. These results hint at the presence of a maturity-stability balance in DENV, and the unfavorable acidic residues at P3 may play a regulatory role.

% Identity (amino acid)	Human-Furin	Aedes-Furin-like protease 1	Aedes-Vitellogenin Convertase	Aedes-Furin-like protease 2	Aedes-AAEL010725-PA
Human-Furin		39	39	39	33
Aedes-Furin-like protease 1	39		99	42	34
Aedes-Vitellogenin Convertase	39	99		42	34
Aedes-Furin-like protease 2	39	42	42		98
Aedes-AAEL010725-PA	33	34	34	98	

Supplementary Figure 2: Amino acid sequence identity matrix of furin and furin-like proteases between human and *Aedes aegypti*.

Using directed-evolution, we tested the fitness of thousands of DENV2 prM cleavage site variants, revealing high sequence plasticity. Predicted cleavage efficiency varied greatly between Vero- and C6/36-selected variants, further indicating differences in substrate preference of mammalian and insect furin which warrant further investigation. We observed many more viable variants in C6/36 cells compared to Vero cells, which may indicate a higher tolerance of mutation in furin sites in insect cells which could drive viral diversity and emergence in nature. However, we cannot rule out that the greater number of viable variants is an artifact of greater efficiency of the DENV reverse genetics system in C6/36 cells. Both of the top Vero- and C6/36-selected variants displayed enhanced growth kinetics and a slight increase in peak titer in Vero cells, indicating tissue culture adaption of the prM cleavage site; this advantage may not be reflected in natural infections or *in vivo*. Alignment of DENV prM sequences indicates that the furin cleavage site is extremely conserved in nature, despite high experimental plasticity. This discrepancy suggests either an unknown advantage of the WT cleavage site or a bottleneck effect in nature. Nevertheless, both variants from our directed evolution experiment are more mature than DV2-WT, suggesting selection for mature DENV2 *in vitro* in both mammalian and inset cells. Future experiments could focus on *in vivo* evolution of the genetic pool, using Aedes aegypti mosquitoes.

Based on a small cohort of monoclonal Abs and anti-DENV serum, our genetically modified mature DENVs show similar neutralization profiles to wildtype against antibodies targeting maturation independent epitopes (such as EDE1, EDE2 and BC loop epitopes), suggesting mutations at the prM cleavage site do not affect the overall viral protein structure. However, maturation dependent epitopes present only in one form of the virus, such as the fusion loop[17], show a different neutralization profile against our mature DENVs. DENV2 has been shown to be very flexible, and "breathing" could account for the insensitivity of 1M7 neutralization to maturation status[38,39]. Our results support earlier studies showing differences in antigenicity between mature and immature DENVs using furin overexpression cells[18], while providing new opportunities for studying the role of maturation in antigenicity, vaccine design, and *in vivo* replication and pathogenesis. Recent studies have demonstrated a potential disconnect between neutralizing antibody correlates of protective immunity in vaccine recipients[40]. Our data are consistent with earlier studies showing that the maturation status of DENV particles could have major implications for neutralization assay outcomes and result in bias during the determination of "correlates of protection" for vaccine studies[17,20,41]. These findings reinforce the importance of monitoring DENV maturation status in vaccine development, and our engineered strains provide a universal way to control DENV maturation for live-attenuated vaccine candidates independent of cell and host.

Like many studies, our report generated additional questions. Biologically, does DENV maturation play a more critical role than simply preventing premature fusion during production? Could maturation also play a role in vector-to-host or host-to-vector transmission? Is fully mature DENV advantageous or deleterious in mosquitoes and mammals? What determinants outside of the primary cleavage site sequence regulate maturation efficiency? Will biologically stabilized virions drive selection of unique subsets of neutralizing antibodies after infection? Clinically, the antigenic differences between mature and immature DENV require more comprehensive investigation. Furthermore, a new class of vaccines could be imagined based on stabilized mature particles which elicit maturation discriminatory antibodies. Given the clinical relevance and enigmatic nature of DENV maturation, our study adds to understanding of DENV maturation control and provides essential tools for future investigations.

Materials and Methods

Cells, plasmids and viruses

Mosquito (*Aedes albopictus*) C6/36 cells (ATCC# CRL-1660) were maintained in minimum essential medium (MEM) (Gibco) media supplemented with 5% fetal bovine serum (FBS) (HyClone), 100 U/mL penicillin and 100 mg/mL penicillin/streptomycin (P/S) (Gibco), 0.1 mM nonessential amino acids (NEAA) (Gibco), HEPES (Gibco) and 2 mM glutaMAX (Gibco) and incubated in the presence of 5% CO_2 at 32°C. Vero (ATCC# CCL-81), VF-Hi and VF-Lo (generated from this study) were maintained in Dulbecco's Modified Eagle's Medium (DMEM) (Gibco) supplemented with 10% FBS, P/S, NEAA and HEPES and incubate in 5% CO_2 at 37°C. DENV variants were generated by site-directed mutagenesis using Q5 High-fidelity DNA polymerase (NEB) followed by DENV reverse genetics (see below). The Env and prM of all DENV variants were sequence confirmed. DV1, 2, 3 and 4-WT viruses are grow in C6/36 or Vero cells maintained in infection media. C6/36 infection media contains Opti-MEM (Gibco) supplemented with 2% FBS, 1% P/S, 0.1 mM NEAA, 1% HEPES and 2 mM glutaMAX. Vero infection media is the same as the growth media except with 2% FBS supplement.

DENV reverse genetics

Recombinant viruses were constructed using a four-plasmid cloning strategy as described previously[42]. The DENV genome was divided into four fragments (A–D fragment) and subcloned into four separate plasmids. A T7 promoter was introduced into the 5' end of the A fragment, and unique type IIS restriction endonuclease cleavage sites are introduced into the 5' and 3' ends of each fragment to allow for systematic assembly into a full-length cDNA from which the full-length RNA transcripts can be derived. Plasmid DNA was grown in Top10 chemical component cells (ThermoFisher), digested with the

corresponding enzymes, gel purified, and ligated together with T4 DNA ligase (NEB). Ligation products were purified by chloroform extraction. The purified ligation product was used as a template for *in-vitro* transcription to generate infectious genome-length capped viral RNA transcripts using T7 RNA polymerase (ThermoFisher). RNA was electroporated into either C6/36 or Vero cells. Cell culture supernatant containing virus was harvested 4 – 5 days post-electroporation as passage zero. During the subsequent passages following infection, the cells were grown in infection media.

Stable cell line generation, VF-Hi and VF-Lo

Human furin was cloned in the sleeping beauty transposon plasmid[26] pSB-bi-RP (Addgene #60513), transfected along with transposase, pCMV(CAT)T7-SB100 (Addgene #34879) into Vero cell using PEI Max (MW 40,000) (Polysciences) and selected with 2.5 µg/ml Puromycin (Gibco). Clonal cell lines were generated through limited dilution of the polyclonal cell line on a 96-well plate at the concentration of 0.3 cell/well.

DENV growth kinetic and quantification

500,000 Vero or C6/36 cells were seeded in each well of a 6-well plate 1 day prior infection. Cells were infected with DENV at 0.05 to 0.1 M.O.I. assuming $1x10^6$ cells on the day of infection. Cells were washed 3 times with PBS and replenished with 3 mL of infection media after 1 hour of inoculation at 37°C in 5% CO_2 incubator. 300 µl of viral supernatant was collected and fresh media was replenished at 0, 24, 48, 72, 96 and 120 hpi and stored at -80°C. Titer of the viral supernatant was determined using a standard DENV foci forming assay. In brief, Vero cells were seeded at $2x10^4$ cells/well in a 96-well plate. 50 µl of serial diluted viral supernatant were added to each well and incubated for 1h at 37°C in 5% CO_2 incubator. 125 µl of overlay (Opti-MEM + 5% methyl cellulose + NEAA + P/S) was added to each well and incubated for 48h at 37°C + 5% CO_2. Each well was rinsed 3 times with PBS and fixed with 10% formalin in PBS for staining. Vero cells were blocked in permeabilization buffer (eBioscience) with 5% non-fat dried milk. Two primary antibodies, anti-prM mAb 2H2 and anti-Env mAb 4G2, from non-purified hybridoma supernatant were used at 1:500 dilution in blocking buffer. Goat anti-mouse secondary conjugated with horseradish peroxidase (HRP) (SeraCare's KPL) were diluted at 1:1000 in blocking buffer. Foci were developed using TrueBlue HRP substrate (SeraCare's KPL) and counted using an automated Immunospot Analyzer instrument (Cellular Technology Limited). All experiments were performed independently a minimum of 3 times.

Immunostaining and western blotting for human furin

Cells were fixed in 10% formalin in PBS and permeabilized with permeabilization buffer (eBioscience). Rabbit anti-furin (Thermo, PA1-062, 1:1000) was used as primary antibody. Goat anti-rabbit Alexa488

(Invitrogen, 1:2000) as secondary antibody. For western blotting, cell were lysed in 1% TritonX100, 100 mM Tris, 2M NaCl and 100 mM EDTA. Cell lysates were run in SDS-PAGE and blotted onto PVDF membrane. Furin bands were detected using rabbit anti-furin polyclonal at 1:1000 and Goat anti-rabbit HRP (Invitrogen, 1:5000) was used as secondary antibody.

Western Blotting for DENV maturation

Viral stocks or supernatant from DENV growth curves at 120hpi were diluted with 4x Laemmli Sample Buffer (Bio-Rad) and boiled at 95°C for 5 minutes. Following SDS-PAGE electrophoresis, proteins were transferred to PVDF membrane and blocked in blocking buffer consist of 3% non-fat milk in PBS + 0.05% Tween-20 (PBS-T). The membrane was incubated with polyclonal rabbit anti-prM (1:1000, Invitrogen, Cat. #PA5-34966) and purified human anti-Env (fusion loop) 1M7 (2µg/ml) in 2% BSA + PBS-T solution for 1h at 37°C. The primary antigen-antibody complex was detected by incubating the blot with goat anti-rabbit IgG HRP (1:10000, Jackson-ImmunoLab) and sheep anti-human IgG HRP (1:5000, GE Healthcare) in 3% milk in PBS-T, for 1h at room temperature. Membranes were developed by Supersignal West Pico PLUS Chemiluminescent Substrate (ThermoFisher). Western blot images were captured with iBright FL1500 imaging system (Invitrogen). The pixel intensity of individual bands was measured using ImageJ, and relative maturation was calculated by using the following equation: $(prM_{Exp}/Env_{Exp})/(prM_{WT}/Env_{WT})$. All experiments were performed independently a minimum of 3 times.

Foci reduction neutralization titer assay (FRNT Assay)

FRNT assays were performed on Vero cells as has been described previously[43]. Briefly, $2x10^4$ Vero cells were seeded in a 96-well plate. Antiserum or mAbs were serially diluted and mixed with DENV viruses (80 – 100 FFU/well) at a 1:1 volume ratio and incubated at 37°C for 1h without the cells. The mixture was transferred to the 96-well plate with Vero cells and incubated at 37°C for 1h. The plate is subsequently overlaid with overlay medium (see above). Viral foci were stained and counted as described above. Data were fitted with variable slope sigmoidal dose-response curves and $FRNT_{50}$ were calculated with top or bottom restraints of 100 and 0, respectively. All experiments were performed independently at least 2 times, due to limited amounts of human serum.

DENV2 library generation and directed-evolution

DENV prM libraries were engineered through saturation mutagenesis on amino acid residues P3, 5, 6 and 7 of the DENV furin cleavage site based on previously published protocol[44]. In brief, degenerate NNK oligos (Integrated DNA Technologies) were used to amplify the prM region to generate a library with mutated prM DNA fragments. To limit bias and ensure accuracy, Q5 high fidelity polymerase (NEB) was used and limited to <18 cycles of amplification. The DNA library was cloned into the DENV reverse genetics system

plasmid A to create a plasmid library by standard restriction digestion. Ligation reactions were then concentrated and purified by ethanol precipitation. Purified ligation products were electroporated into DH10B ElectroMax cells (Invitrogen) and directly plated on multiple 5,245-mm^2 bioassay dishes (Corning) to avoid bias from bacterial suspension cultures. Colonies were pooled and purified using a Maxiprep Kit (Qiagen). The plasmid library was used for DENV reverse genetics as described above. The *in vitro* transcribed DENV RNA library was electroporated in either Vero or C6/36 cells, the viral supernatants were passaged 3 times every 4 to 5 days in the corresponding cells for enrichment.

High-throughput sequencing and analysis

Viral RNA was isolated using a QIAamp Viral RNA Mini Kit (Qiagen). Amplicons containing the library regions were prepared for sequencing through two rounds of PCR, using the Illumina TruSeq system and Q5 Hot Start DNA polymerase (NEB). Primers for the first round of PCR were specific to the DENV2 prM sequence with overhangs for Illumina adapters. This PCR product was purified and used as a template for a second round of PCR using the standard Illumina P5 and P7 primers with barcodes and sequencing adaptors. PCR products were purified and analyzed on a Qubit 4 fluorometer (Invitrogen) and Bioanalyzer (Agilent Technologies) for quality control. Amplicon libraries were diluted to 4 nM and pooled for sequencing, which was carried out on a MiSeq system with 300bp paired-end reads. Plasmid and P0 libraries were sequenced at a depth of ~1 million reads per sample; further passages were sequenced with depth between 300,000 – 1 million reads to sample. A custom perl script[44] was used to analyze the sequences, and custom R scripts were used to plot the data.

Furin cleavage prediction

Furin cleavage site efficiency was predicted using the Pi-Tou software[25], providing amino acids from position P14-P6' of the DENV furin cleavage sites.

Statistical analysis

Statistical analysis was carried out using Graphpad Prism version 9.0. Growth kinetics and maturation of DENV variants were compared to their corresponding wildtype using 2-way ANOVA multiple comparisons. Neutralization titers of DENV variants were compared to their corresponding wildtype using Student's t-test. Significance symbols are defined as follow: * $p<0.05$, ** $p< 0.01$, *** $p<0.001$, **** $p<0.0001$. Data are graphed as mean +/- standard deviation.

Acknowledgments

We thank members of the Baric and de Silva laboratories for helpful discussions. This project received support from NIH grants AI107731 and AI125198 to A.M.D and R.S.B. P01 AI106695 to A.M.D.. L.V.T. is the recipient of the Pfizer NCBiotech Distinguished Postdoctoral Fellowship in Gene Therapy.

Author Contributions

L.V.T and R.S.B designed the study. R.M.M perform high-throughput sequencing preparation and analysis. L.V.T., R.M.M., S.D., L.E.A., L.J.W. performed experiments. L.V.T., A.M.D., R.S.B. provide oversight of the project. L.V.T. wrote the manuscript. R.M.M and R.S.B. reviewed and revised the final version.

Conflict of Interest

L.V.T. R.M.M. and R.S.B. are inventors on a patent application filed on the subject matter of this manuscript.

References

1. Brady, O. J. *et al.* Refining the Global Spatial Limits of Dengue Virus Transmission by Evidence-Based Consensus. *PLoS Negl. Trop. Dis.* **6**, (2012).
2. Bhatt, S. *et al.* The global distribution and burden of dengue. *Nature* **496**, 504–507 (2013).
3. Messina, J. P. *et al.* The current and future global distribution and population at risk of dengue. *Nat. Microbiol.* **4**, 1508–1515 (2019).
4. Wilder-Smith, A. *et al.* Deliberations of the Strategic Advisory Group of Experts on Immunization on the use of CYD-TDV dengue vaccine. *Lancet Infect. Dis.* **19**, e31–e38 (2019).
5. Report, W. H. O. Dengue vaccine: WHO position paper, September 2018 – Recommendations. *Vaccine* **37**, 4848–4849 (2019).
6. White, J. M., Delos, S. E., Brecher, M. & Schornberg, K. Structures and mechanisms of viral membrane fusion proteins: Multiple variations on a common theme. *Crit. Rev. Biochem. Mol. Biol.* **43**, 189–219 (2008).
7. Harrison, S. C. Viral membrane fusion. *Virology* **479–480**, 498–507 (2015).
8. Kuhn, R. J. *et al.* Structure of dengue virus: implications for flavivirus organization, maturation, and fusion. *Cell* **108**, 717–25 (2002).
9. Zybert, I. A., van der Ende-Metselaar, H., Wilschut, J. & Smit, J. M. Functional importance of dengue virus maturation: Infectious properties of immature virions. *J. Gen. Virol.* **89**, 3047–3051 (2008).

475 10. Plevka, P., Battisti, A. J., Sheng, J. & Rossmann, M. G. Mechanism for maturation-related
476 reorganization of flavivirus glycoproteins. *J. Struct. Biol.* **185**, 27–31 (2014).
477 11. Kostyuchenko, V. A., Zhang, Q., Tan, J. L., Ng, T.-S. & Lok, S.-M. Immature and Mature Dengue
478 Serotype 1 Virus Structures Provide Insight into the Maturation Process. *J. Virol.* **87**, 7700–7707
479 (2013).
480 12. Zhang, Y. *et al.* Conformational changes of the flavivirus E glycoprotein. *Structure* **12**, 1607–1618
481 (2004).
482 13. Mackenzie, J. M. & Westaway, E. G. Assembly and Maturation of the Flavivirus Kunjin Virus
483 Appear To Occur in the Rough Endoplasmic Reticulum and along the Secretory Pathway,
484 Respectively. *J. Virol.* **75**, 10787–10799 (2001).
485 14. Li, L. *et al.* The flavivirus precursor membrane-envelope protein complex: structure and
486 maturation. *Science* **319**, 1830–1834 (2008).
487 15. Yu, I. *et al.* Structure of the Immature Dengue Virus at Low pH Primes Proteolytic Maturation. **13**,
488 1834–1838 (2008).
489 16. Wirawan, M. *et al.* Mechanism of Enhanced Immature Dengue Virus Attachment to Endosomal
490 Membrane Induced by prM Antibody. *Structure* **27**, 253-267.e8 (2019).
491 17. Raut, R. *et al.* Dengue type 1 viruses circulating in humans are highly infectious and poorly
492 neutralized by human antibodies. *Proc. Natl. Acad. Sci.* **116**, 227–232 (2019).
493 18. Dowd, K. A., Mukherjee, S., Kuhn, R. J. & Pierson, T. C. Combined Effects of the Structural
494 Heterogeneity and Dynamics of Flaviviruses on Antibody Recognition. *J. Virol.* **88**, 11726–11737
495 (2014).
496 19. Galula, J. U., Salem, G. M., Chang, G. J. J. & Chao, D. Y. Does structurally-mature dengue virion
497 matter in vaccine preparation in post-Dengvaxia era? *Hum. Vaccines Immunother.* **15**, 2328–2336
498 (2019).
499 20. Pierson, T. C. & Diamond, M. S. Degrees of maturity: The complex structure and biology of
500 flaviviruses. *Curr. Opin. Virol.* **2**, 168–175 (2012).
501 21. Rodenhuis-Zybert, I. A. *et al.* Immature dengue virus: A veiled pathogen? *PLoS Pathog.* **6**, (2010).
502 22. Katzelnick, L. C. *et al.* Immune correlates of protection for dengue: State of the art and research
503 Agenda. *Vaccine* **35**, 4659–4669 (2017).
504 23. Mukherjee, S. *et al.* Enhancing dengue virus maturation using a stable furin over-expressing cell
505 line. *Virology* **497**, 33–40 (2016).
506 24. Gallichotte, E. N. *et al.* Genetic Variation between Dengue Virus Type 4 Strains Impacts Human

Antibody Binding and Neutralization. *Cell Rep.* **25**, 1214–1224 (2018).

25. Tian, S., Huajun, W. & Wu, J. Computational prediction of furin cleavage sites by a hybrid method and understanding mechanism underlying diseases. *Sci. Rep.* **2**, (2012).
26. Kowarz, E., Löscher, D. & Marschalek, R. Optimized Sleeping Beauty transposons rapidly generate stable transgenic cell lines. *Biotechnol. J.* 647–653 (2015). doi:10.1002/biot.201400821
27. Dejnirattisai, W. *et al.* A new class of highly potent, broadly neutralizing antibodies isolated from viremic patients infected with dengue virus. *Nat. Immunol.* **16**, 170–177 (2015).
28. Smith, S. A. *et al.* The potent and broadly neutralizing human dengue virus-specific monoclonal antibody 1C19 reveals a unique cross-reactive epitope on the bc loop of domain II of the envelope protein. *MBio* **4**, 1–12 (2013).
29. Matthews, D. J., Goodman, L. J., Gorman, C. M. & Wells, J. A. A survey of furin substrate specificity using substrate phage display. *Protein Sci.* **3**, 1197–1205 (1994).
30. Izidoro, M. A. *et al.* A study of human furin specificity using synthetic peptides derived from natural substrates, and effects of potassium ions. *Arch. Biochem. Biophys.* **487**, 105–114 (2009).
31. Shiryaev, S. A. *et al.* High-Resolution Analysis and Functional Mapping of Cleavage Sites and Substrate Proteins of Furin in the Human Proteome. *PLoS One* **8**, 1–12 (2013).
32. Duckert, P., Brunak, S. & Blom, N. Prediction of proprotein convertase cleavage sites. *Protein Eng. Des. Sel.* **17**, 107–112 (2004).
33. Cano-Monreal, G. L., Williams, J. C. & Heidner, H. W. An arthropod enzyme, Dfurin1, and a vertebrate furin homolog display distinct cleavage site sequence preferences for a shared viral proprotein substrate. *J. Insect Sci.* **10**, 1–16 (2010).
34. Snapp, E. L. *et al.* Structure and topology around the cleavage site regulate post-translational cleavage of the HIV-1 gp160 signal peptide. *Elife* **6**, 1–25 (2017).
35. Tse, L. V., Hamilton, A. M., Friling, T. & Whittaker, G. R. A Novel Activation Mechanism of Avian Influenza Virus H9N2 by Furin. *J. Virol.* **88**, 1673–1683 (2014).
36. Zhang, Q. *et al.* The stem region of premembrane protein plays an important role in the virus surface protein rearrangement during dengue maturation. *J. Biol. Chem.* **287**, 40525–40534 (2012).
37. Shen, W.-F. *et al.* Epitope resurfacing on dengue virus-like particle vaccine preparation to induce broad neutralizing antibody. *Elife* **7**, 1–24 (2018).
38. Fibriansah, G. *et al.* Structural Changes in Dengue Virus When Exposed to a Temperature of 37 C. *J. Virol.* **87**, 7585–7592 (2013).

539 39. Kuhn, R. J., Dowd, K. A. & Post, C. B. Shake, rattle, and roll: Impact of the dynamics of flavivirus
540 particles on their interactions with the host. *Virol. J.* 508–517 (2016).
541 doi:10.1016/j.virol.2015.03.025.Shake
542 40. Villar, L. *et al.* Efficacy of a Tetravalent Dengue Vaccine in Children in Latin America. *N. Engl. J.*
543 *Med.* **372**, 113–123 (2015).
544 41. de Silva, A. M. & Harris, E. Which dengue vaccine approach is the most promising, and should we
545 be concerned about enhanced disease after vaccination?: Questions raised by the development
546 and implementation of dengue vaccines: Example of the sanofi pasteur tetravalent dengue
547 vaccine. *Cold Spring Harb. Perspect. Biol.* **10**, 1–11 (2018).
548 42. Messer, W. B. *et al.* Development and characterization of a reverse genetic system for studying
549 dengue virus serotype 3 strain variation and neutralization. *PLoS Negl. Trop. Dis.* **6**, (2012).
550 43. Young, E. *et al.* Identification of Dengue Virus Serotype 3 Specific Antigenic Sites Targeted by
551 Neutralizing Human Antibodies. *Cell Host Microbe* **27**, 710-724.e7 (2020).
552 44. Tse, L. V. *et al.* Structure-guided evolution of antigenically distinct adeno-associated virus variants
553 for immune evasion. *Proc. Natl. Acad. Sci.* **114**, E4812–E4821 (2017).
554